PRAMANA
— journal of
physics

Vol. 83, No. 5
November 2014
pp. 661–671

Describing one- and two-neutron halos in effective field theory

DANIEL R PHILLIPS
Department of Physics and Astronomy and Institute of Nuclear and Particle Physics,
Ohio University, Athens, OH 45701, USA
E-mail: phillips@phy.ohiou.edu

DOI: 10.1007/s12043-014-0862-y; ***e*Publication:** 1 November 2014

Abstract. In this paper, the recent work our group has undertaken on effective field theory (EFT) analyses of experimental data pertaining to one- and two-neutron halo nuclei is discussed. The cases of ^{19}C and ^{8}Li (one-neutron halos) and ^{22}C (two-neutron halo) are considered. For ^{19}C and ^{8}Li electromagnetic processes, such as Coulomb dissociation and radiative capture are considered. In the ^{22}C system the way in which the measured matter radius can be used to derive constraints on the two-neutron separation energy of this very neutron-rich system is shown. In each case the Halo EFT's ability to correlate different experimental observables with one another, in a model-independent manner, and up to an accuracy that is determined by the separation of scales in the halo system is shown.

Keywords. Halo nuclei; effective field theory; radiative capture; Coulomb dissociation.

PACS Nos 25.20.−x; 25.40.Lw; 11.10.Ef; 21.10.Jx; 21.60.De

1. Introduction

Effective field theory (EFT) enables a model-independent, systematically improvable treatment of systems in which a separation of scales exists. Halo nuclei are amenable to an EFT description, because the typical distances occupied by neutrons in a nuclear halo, $R_{\rm halo}$, are much larger than the size of the nuclear core, $R_{\rm core}$. Halo EFT is thus built on the scale hierarchy $R_{\rm core} \ll R_{\rm halo}$. Physical observables in this EFT are expressed as expansions in powers of $R_{\rm core}/R_{\rm halo}$. For nuclei, in which the halo consists of a single neutron it is a simple extension of the EFT for shallow s-wave bound states developed in, e.g., [1–4] – indeed, from the Halo-EFT point of view the deuteron is the lightest halo nucleus, with $R_{\rm core}$ set by the pion Compton wavelength. In the context of few-nucleon systems such an EFT treatment, based on nucleon degrees of freedom interacting via short-range potentials, has been successfully applied not just to the $A = 2$ system, but also to $A = 3$ and $A = 4$ [5–7].

Halo systems beyond $A = 4$ can be treated in an analogous fashion, in which a tightly-bound nuclear core is employed as one degree of freedom. The core is structureless in the leading-order (LO) Halo-EFT Lagrangian, and so the theory is designed to treat reactions in which core structure is not resolved, i.e., momenta are $k \lesssim 1/R_{\rm core}$. Given reasonable values for $R_{\rm core}$, this means that we are restricted to systems with neutron separation energies of 1 MeV or less, but within that domain an EFT treatment that links phenomena across different halos is possible. The formalism was extended to bound states and low-energy resonances of p-wave character in [8]. It has now been applied to numerous halo systems including ^{5}He [8], ^{8}Li [9], ^{15}C [10], and a variety of two-neutron ($2n$) halos [11,12].

In [13] we applied this theory to the one-neutron ($1n$) halo ^{11}Be. This nucleus is particularly interesting because it has both a shallow s-wave ($1/2^+$) and a shallow p-wave ($1/2^-$) bound state. In Halo EFT these bound states are generated by zero-range forces, and thus have (reduced) wave functions

$$u_0(r) = A_0 \exp(-\gamma_0 r), \quad u_1(r) = A_1 \left(1 + \frac{1}{\gamma_1 r}\right) \exp(-\gamma_1 r) \tag{1}$$

with $\gamma_{0,1} = \sqrt{2m_R S_{1n}}$ being the binding momentum of the neutron in the $1/2^{+,-}$ state and $A_{0,1}$, the corresponding asymptotic normalization coefficient (ANC). At leading order (LO), the ANC (A_0) is fixed to be $\sqrt{2\gamma_0}$, and so there are three free parameters in the theory at LO: γ_0, γ_1, and A_1. Data on the energy levels of ^{11}Be fix the first two, and the third was determined using the sizeable and well-measured $B(E1)$ of the $1/2^+$ to $1/2^-$ transition in ^{11}Be. In future this parameter could perhaps be extracted from *ab-initio* calculations (see §3). Once these three parameters were fixed we could predict the Coulomb dissociation spectrum of ^{11}Be at next-to-leading order (NLO) in Halo EFT. At that order, an additional parameter associated with the ANC (A_0) is introduced. This can be adjusted to obtain a good description of the low-energy $\mathrm{d}B(E1)/\mathrm{d}E$ spectrum [13].

While the zero-range wave functions (1) are the starting point for the Halo EFT expansion, expressions are systematically corrected to include the piece of the dissociation (or capture) which takes place at distances where the expressions (1) do not apply, $r \sim R_{\rm core}$. For Coulomb dissociation of ^{11}Be this piece of the matrix element is parametrically suppressed by $(R_{\rm core}/R_{\rm halo})^2$. Thus, the dominant effect of dissociation at distances $\sim R_{\rm core}$ appears one order beyond that to which the computation was carried out in [13]: at N^{2}LO there is an unknown low-energy constant (LEC) in the Halo EFT photodissociation amplitude, which can only be determined using the data on $E1$ transitions in ^{11}Be.

Section 2 describes the recent results from a similar treatment of the s-wave $1n$ halo ^{19}C. Fitting the N^{2}LO EFT amplitude for the Coulomb dissociation of ^{19}C to experimental data allows accurate values to be extracted for the n^{18}C effective-range parameters [14]. Such treatments are similar to those based on effective-range theory (e.g., [15]), but offer the added benefit of a systematic EFT expansion which permits estimation of the error associated with the neglected terms.

The reaction $^7\mathrm{Li} + n \to {}^8\mathrm{Li} + \gamma$ involves capture of a neutron into a p-wave halo state. There have been many attempts to describe this process theoretically, mainly driven by its relation to a key process in the chain of solar neutrino production reactions, $^7\mathrm{Be} + p \to {}^8\mathrm{B} + \gamma$. An accurate EFT description of these $A = 8$ radiative captures becomes difficult as several inputs are already required at LO. Section 3 describes one way to deal

with the issue: the use of ANCs obtained in *ab-initio* calculations as input to Halo EFT. The resulting predictions for capture reactions agree with the data to within the expected accuracy of a LO calculation in the EFT [16].

Two-neutron halos are discussed in §4. A recent measurement by Tanaka *et al* of the r.m.s. matter radius of ^{22}C gives $\langle r_m^2\rangle^{1/2} = 5.4 \pm 0.9$ fm [17]. Here, how the Halo EFT predicts a universal correlation between the matter radius and the two-neutron separation energy of s-wave $2n$ halos, such as ^{22}C is shown. Applying this universal relation to ^{22}C and including estimates of higher-order EFT corrections in a treatment where ^{20}C is an inert core, we have put constraints on the poorly-known values of the ^{22}C two-neutron separation energy and n^{20}C virtual-state energy using the experimental datum [18]. Finally, §5 offers a few concluding remarks.

2. Coulomb dissociation of ^{19}C

The ^{18}C ground state has $J^\pi = 0^+$, while the ground state of ^{19}C is now understood to be $1/2^+$ and has a one-neutron separation energy of ≈500 keV. This is significantly less than the one-neutron separation energy of ^{18}C: $S_{1n}(^{18}\mathrm{C}) = 4.2$ MeV. ^{19}C is thus, a candidate for an s-wave neutron-halo state: it has a reasonable separation of scales, with the expansion parameter $R_{\rm core}/R_{\rm halo}$ expected to be ≈0.4.

In [14] we have derived the dipole transition strength, $B(E1)$, for the excitation of ^{19}C to the $^{18}\mathrm{C} + n$ continuum. We found [10]

$$\frac{\mathrm{d}B(E1)}{e^2\mathrm{d}E} = \frac{12}{\pi^2}\frac{\mu^3}{M^2}Z^2\frac{\gamma_0}{1-r_0\gamma_0}\frac{p^3}{(\gamma_0^2+p^2)^4}, \tag{2}$$

where r_0 is the effective range of the n^{18}C interaction. Up to the accuracy of the calculation of [14], r_0 is related to the ANC (A_0) by

$$A_0^2 = \frac{2\gamma_0}{1-\gamma_0 r_0}. \tag{3}$$

At LO in the EFT $r_0 = 0$ and eq. (2) is universal, i.e., it applies to any s-wave $1n$ halo at LO, and, indeed, to the dissociation of any shallow s-wave quantum bound state. Effects of the finite range of the ^{18}C–n interaction appear at orders beyond leading, and are manifest in eq. (2) through the effective range parameter r_0. In the case of ^{19}C, p-wave final-state interactions are strongly suppressed, they do not appear until N^{3}LO in the EFT expansion (cf. the case of ^{11}Be). Short-distance ($\sim R_{\rm core}$) pieces of the capture matrix element occurs only at N^{4}LO [19].

Therefore, by combining eq. (2) and a reaction theory that relates $\mathrm{d}B(E1)/\mathrm{d}E$ to the Coulomb dissociation cross-section (see, e.g., [20] for a full procedure and [14] for a summary), we can predict the Coulomb dissociation cross-section at N^{2}LO in the EFT. In practice we have fitted the input parameters γ_0 and r_0 to the data on the differential angular and differential energy cross-sections for Coulomb dissociation of ^{19}C from [21] and [22]. In figure 1 we show these data along with the best fits. In each of the panels the dashed lines are fits to just the data shown in that panel. The solid line is the combined fit. The agreement is very good and extends beyond the fit region $E < 1$ MeV.

The best fit to the combined data set yields $r_0/a = 0.33$ for the ratio of ^{18}C–n effective range to scattering length. This is a more accurate value for the EFT expansion parameter

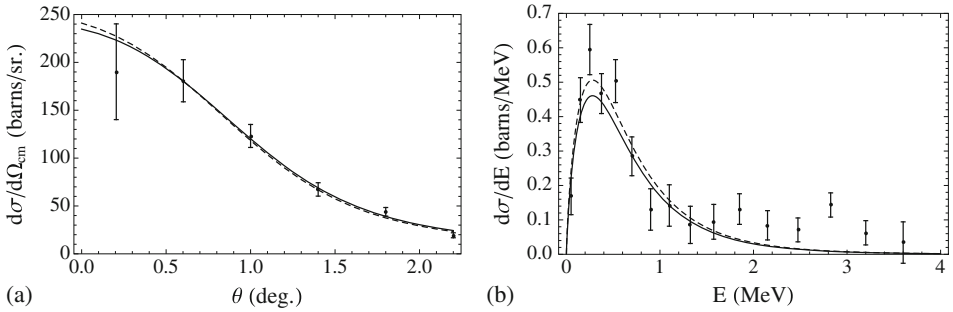

Figure 1. (**a**) Angular distribution of the differential cross-section for $S_{1n}(^{19}\mathrm{C}) = 540$ keV (dashed line) and $S_{1n}(^{19}\mathrm{C}) = 575$ keV (solid line) (data from [21]). (**b**) Relative energy spectrum of the differential cross-section at $S_{1n}(^{19}\mathrm{C}) = 580$ keV (dashed line) and $S_{1n}(^{19}\mathrm{C}) = 575$ keV (solid line) (data from [22]) (figure taken from [14]).

than our initial estimate $R_{\mathrm{core}}/R_{\mathrm{halo}} \approx 0.4$. Therefore, in addition to the statistical errors, all the parameters determined above have a relative error of $r_0^3/a^3 = 0.036$. The EFT extraction gives values of $S_{1n}(\,^{19}\mathrm{C})$, a, and r_0 of $(575 \pm 55(\mathrm{stat.}) \pm 20(\mathrm{EFT}))$ keV, $(7.75 \pm 0.35(\mathrm{stat.}) \pm 0.3(\mathrm{EFT}))$ fm, and $(2.6^{+0.6}_{-0.9}(\mathrm{stat.}) \pm 0.1(\mathrm{EFT}))$ fm, respectively. Note that uncertainties in the reaction theory must be assessed separately [23].

The width of the longitudinal momentum distribution predicted by EFT using these parameters also agrees well with the experimental data of Bazin *et al* [24]. The success of this description affirms the dominance of the s-wave configuration of the valence neutron.

3. Threshold neutron capture on ^{7}Li

Halo EFT was applied to the $A = 8$ capture process $^7\mathrm{Li}(n, \gamma)^8\mathrm{Li}$ in [9]. The neutron and ^{7}Li core were the degrees of freedom used in the LO calculation. Four parameters were needed as input and in ref. [9] a combination of capture and scattering length data and model assumptions were used to fix them.

In [16] we pursued an alternative strategy. We used ANCs from *ab-initio* calculations to fix several EFT parameters. We also incorporated the bound excited state of ^{7}Li (^{7}Li* hereafter) as an additional degree of freedom in the EFT. The high-energy scale in our EFT can then be associated with the breakup energy of $^7\mathrm{Li} \to t + {}^4\mathrm{He}$. From the binding energy of ^{8}Li with respect to the ^{7}Li–n threshold, 2.03 MeV, we obtain a nominal expansion parameter ~ 0.5. However, the result we ultimately find for the p-wave effective range in n^7Li scattering suggests a more convergent expansion.

There are two different incoming spin channels $S_i = 2, 1$ in this process. As spin does not participate in the $E1$ transition the ANCs for each ^{8}Li state is considered (^{8}Li and ^{8}Li*) with respect to both the n^7Li spin channels. This necessitates the computation of four ANCs, results of which are given in table 1. These were obtained via variational Monte Carlo calculations using the Argonne v18 NN potential and UIX 3N force [25]. Overall, the agreement with the experimental data of [26] is remarkable. The inclusion of the excited state of ^{7}Li as an extra degree of freedom signifies the need of the ANC of both ^{8}Li and ^{8}Li* in $^7\mathrm{Li}^* + n$ channels. Those three ANCs have not been determined

Table 1. ANCs ($\text{fm}^{-1/2}$) for different channels. The $\tilde{C}_{(X)}$ represents ANCs of the bound excited state of ^{8}Li. The first row gives the variational Monte Carlo $^7\text{Li} + n$ ANCs reported in [25] and the second row shows measurements by Trache *et al.*

	$C_{(^3P_2)}$	$C_{(^5P_2)}$	$\tilde{C}_{(^3P_1)}$	$\tilde{C}_{(^5P_1)}$
Nollett	−0.283(12)	−0.591(12)	0.220(6)	0.197(5)
[26]	−0.284(23)	−0.593(23)	0.187(16)	0.217(13)

experimentally, but can be computed by the methods discussed in [25]. From the ANCs and Halo EFT formulae that relate them to scattering parameters, we find an effective 'range' for n^7Li scattering in the channel where ^{8}Li occurs at $r_1 = -1.43\ \text{fm}^{-1}$.

With the input parameters fixed, we can predict the capture to the ground state of ^{8}Li. The scattering length in the $^5S_2$ n^7Li channel is significantly larger than R_{core}, and so the EFT mandates resummation of the initial-state interactions in that channel (see figure 2). In contrast, the scattering length in the $^3S_1$ channel is 'natural' (i.e., $a \sim R_{\text{core}}$) and so initial-state interactions in that channel only appear at NLO. The nominal accuracy of the LO cross-section prediction, which is shown in figure 3, is ≈40%. The central value of the threshold cross-section is below the average data, but within the expected size of higher-order corrections. In fact, because at NLO there are increases in the ANCs used in the EFT calculation, we expect the NLO Halo-EFT result for the cross-section to be higher than the LO prediction.

We can also compute the fraction of the capture that proceeds from the initial $S_i = 2$ state. We find

$$\frac{\sigma[(S_i = 2) \to 2^+]}{\sigma(\to 2^+)} = 0.93(2), \tag{4}$$

where the uncertainty comes from the higher-order effects in the EFT. In [27] (see also [28]), a lower bound of 0.86 for the ratio on the left-hand side of eq. (4) has been reported.

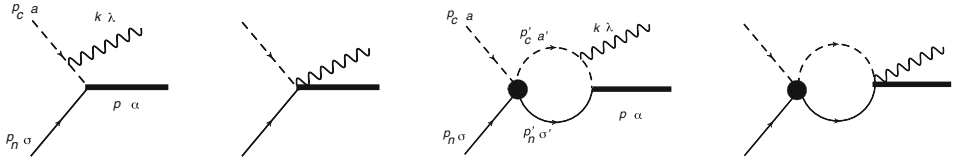

Figure 2. Tree and loop diagrams for neutron capture to ^{8}Li and ^{8}Li*. The solid line represents the neutron, the dashed line the ^{7}Li core, and the thick solid line ^{8}Li (or ^{8}Li*). The two left-most diagrams are LO for two initial total spin $S_i = 2$ and $S_i = 1$ channels. The dominant components in the initial state are $^5S_2$ and $^3S_1$ but d-wave components also contribute in the left diagram. The black blob corresponds to the scattering of the incoming particles in the s-wave. The sum of the two right-most diagrams is finite, as a result of current conservation [9,13]. For these two diagrams only the $S_i = 2$ channel occurs at LO. Perturbative initial-state scattering effects in the $S_i = 1$ channel enter at NLO. With the ^{7}Li fields in the loop changed to ^{7}Li* fields, these diagrams represent the first dynamical effect of core excitation that takes place (it occurs at NLO). Detailed discussions can be found in [16] (figures taken from [16]).

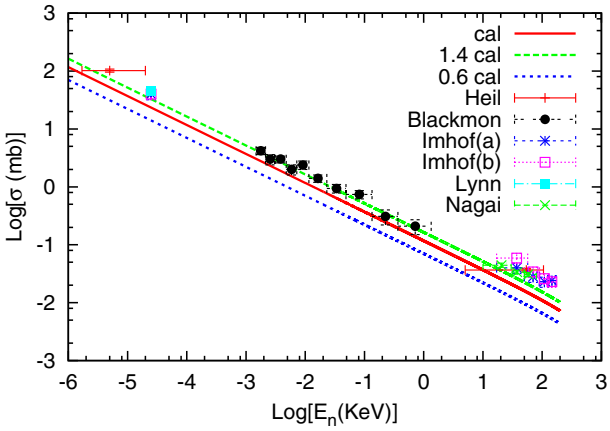

Figure 3. Total cross-section vs. neutron laboratory energy and various data (for details of data, see [16]). 'cal' is our LO results, while '1.4cal' and '0.6cal' are the LO results multiplied by 1.4 and 0.6, to indicate our LO theory uncertainty (figure taken from [16]).

Our result is certainly consistent with that constraint. In contrast, the EFT calculation in [9] assumed equal n ^{7}Li coupling strengths in $^3P_2$ and $^5P_2$ channels and consequently failed to satisfy the experimental lower bound.

As for the branching ratio for capture to the ground state, we find that near threshold the ratio is $\sigma(\to 2^+)/\sigma = 0.88$, with the remaining 12% going to the excited (1^+) state in ^{8}Li. This ratio is largely controlled by the excited- and ground-state ANCs, but is also affected by the initial-state (rescattering) effect due to the large ($\sim R_{\rm halo}$) s-wave scattering length in the $S_i = 2$ channel. In [29], the branching ratio is measured to be 0.89 ± 0.01 for thermal neutrons. The authors of [30] also recorded the same value at 20 to 70 keV. Both these measurements are in excellent agreement with our result.

We have subsequently extended this approach to describe the isospin-mirror reaction $^7\mathrm{Be} + p \to {}^8\mathrm{B} + \gamma$. The Halo EFT is even more convergent in this reaction, because the ^{8}B ground state is shallower than that of ^{8}Li. For centre-of-mass energies below 400 keV, the resulting description of the astrophysical S-factor is already quite accurate at LO [31].

4. The matter radius of ^{22}C

Recently, Tanaka *et al* measured the reaction cross-section of ^{22}C on a hydrogen target and, using Glauber calculations, deduced a ^{22}C r.m.s. matter radius of 5.4 ± 0.9 fm [17]. Their measurement implies that the two valence neutrons in ^{22}C preferentially occupy the $1s_{1/2}$ orbital and are weakly bound [17]. This conclusion is supported by the data on high-energy two-neutron removal from ^{22}C [32]. As ^{21}C is unbound [33], it suggests that ^{22}C is an s-wave Borromean halo nucleus with two neutrons orbiting a ^{20}C core.

EFT was applied to $2n$ halo nuclei in [11] and equations that describe the core–neutron–neutron bound state were derived. These are the (homogeneous) Faddeev

equations for this three-body system. The equations require two-body subsystem amplitudes as input. To solve the Faddeev equations an ultraviolet cut-off, Λ, needs to be applied to the integrals. A neutron–neutron–core contact interaction, $H(\Lambda)$, is then required to cancel the dependence of physical observables on Λ [34]. Once $H(\Lambda)$ is fixed to an experimental datum, the Faddeev components are independent of the cut-off Λ for momenta $\ll\Lambda$. The resulting theory displays a discrete scale invariance which is related to the Efimov effect [35]. With the Faddeev components in hand, the three-body wave function can be reconstructed and a number of different form factors obtained in the usual way (see [11,18] for details).

Because proper renormalization of this problem requires a three-body force at LO, the inputs to the equations describing an s-wave $2n$ halo are the energies of the neutron–core resonance/bound state, $E_{\rm nc}$, and the nn virtual state, as well as the binding energy, B, of the halo nucleus [35a]. All other properties of the nucleus are predicted (at LO accuracy) once these (together with the core-neutron mass ratio A) are specified.

In [18], we used this methodology to compute the function that describes the mean-square matter radius of an arbitrary Borromean $2n$ halo. We then specialized that result to ^{22}C. The connection between the binding energy and several low-energy properties of ^{22}C, including the r.m.s. matter radius has been explored in a three-body model by Ershov *et al* [36]. Yamashita and collaborators investigated such correlations in halo nuclei earlier in 2004 [37] (see also [38] for a review). In 2011, Yamashita *et al* [39] attempted to apply EFT to analyse the experiment of [17]. However, as discussed in [18], an additional assumption in [39] renders the results of Yamashita *et al* model-dependent – in contrast to the rigorous, model-independent LO-EFT results we discussed here.

From the form factors computed via reconstruction of the nnc wave function, we extract the mean-square radii that describe the quantum-mechanical arrangement of the system. In particular, the mean-square matter radius of a two-neutron halo in the point-like core approximation, $\langle r_0^2\rangle$, can be expressed in terms of such radii as

$$\langle r_0^2\rangle = \frac{2(A+1)^2}{(A+2)^3}\langle r_{n\text{-}nc}^2\rangle + \frac{4A}{(A+2)^3}\langle r_{c\text{-}nn}^2\rangle. \tag{5}$$

At LO in Halo EFT, the quantity $mB\langle r_0^2\rangle$ depends on all the variables featuring in the Faddeev equations: $E_{\rm nn}$, $E_{\rm nc}$, B, and A, but being dimensionless, it can only be a function of dimensionless ratios of these four parameters. Thus, it is convenient to define the function $f\,(E_{\rm nn}/B, E_{\rm nc}/B; A)$ as [37]

$$mB\langle r_0^2\rangle \equiv f\left(\frac{E_{\rm nn}}{B}, \frac{E_{\rm nc}}{B}; A\right). \tag{6}$$

The function f can be calculated for any value of A, but, to be specific, figure 4 shows a three-dimensional plot of $f\,(E_{\rm nn}/B, E_{\rm nc}/B; 20)$ in the $(E_{\rm nn}/B, E_{\rm nc}/B)$ plane. The disagreement with the results of [39] is 15% in the limit $E_{\rm nn} = E_{\rm nc} = 0$ and appears to be worse at finite values of $E_{\rm nc}$ and $E_{\rm nn}$.

Figure 4 gives the results required to set a model-independent constraint on the binding energies of ^{21}C and ^{22}C. First, though, we must account for the fact that, when applied to this system, Halo EFT only reliably predicts the difference between the ^{22}C matter radius

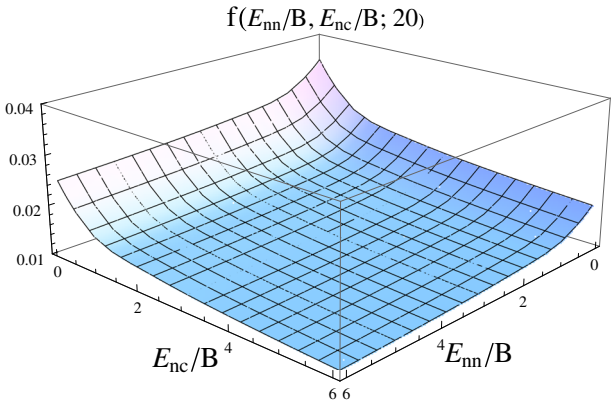

Figure 4. $f\,(E_{\rm nn}/B,\, E_{\rm nc}/B;\, 20)$ vs. $(E_{\rm nn}/B,\, E_{\rm nc}/B)$.

and that of ^{20}C. We account for the finite spatial extent of the core by including that effect in the expression for the mean-square matter radius of the two-neutron halo:

$$\langle r^2\rangle = \langle r_0^2\rangle + \frac{A}{A+2}\langle r^2\rangle_{\rm core}. \tag{7}$$

Here $\langle r^2\rangle_{\rm core}$ is the mean-square radius of the core, which is obtained from the ^{20}C r.m.s. radius of (2.98 ± 0.05) fm measured by Ozawa *et al* [40]. In subsequent calculations, the value of $E_{\rm nn}$ obtained from $a_{\rm nn} = (-18.7 \pm 0.6)$ fm [41] is also used.

To calculate the breakdown scale of the EFT, Λ_0, we approximate the range of the neutron–core interaction by the size of the ^{20}C r.m.s. radius, i.e., we take $\Lambda_0 \approx 1/\sqrt{\langle r^2\rangle_{^{20}\rm C}}$. We then estimate the relative error of the calculation by $\sqrt{mE_{\rm nn}}/\Lambda_0$, $\sqrt{2mE_{\rm nc}}/\Lambda_0$ or $\sqrt{2mB}/\Lambda_0$, whichever is the largest. In figure 5 we plot the sets of $(B,\, E_{\rm nc})$ values that cover the 1-σ range of Tanaka *et al*'s value – $\sqrt{\langle r^2\rangle} = 4.5$, 5.4 and 6.3 fm – in each

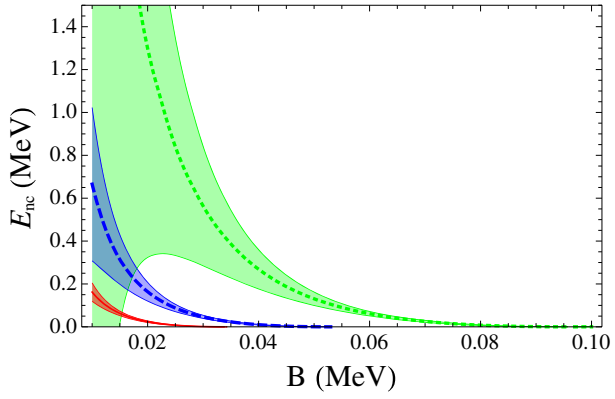

Figure 5. Plots of $\sqrt{\langle r^2\rangle} = 5.4$ fm (blue dashed), 6.3 fm (red solid), and 4.5 fm (green dotted), with their theoretical error bands in the $(B,\, E_{\rm nc})$ plane (figure taken from [18]).

case with a theoretical error band assigned. Since Yamashita *et al* obtained a LO matter radius that is too large for a given binding energy, their constraints on the maximum possible value of B are about 20% weaker than the value obtained in this study.

Figure 5 shows that, regardless of the value of the ^{21}C virtual energy, Tanaka *et al*'s experimental result puts a model-independent upper limit of 100 keV on the $2n$ separation energy of ^{22}C. The recent experimental finding of Mosby *et al* [42] that there is no low-energy resonance in the ^{21}C system puts significant tension into this analysis, suggesting that ^{22}C is bound by less than 20 keV (1-σ, combined EFT, and experimental errors).

Following [11], we can also construct a region in the (B, $E_{\rm nc}$) plane within which an excited Efimov state in ^{22}C could occur. The Efimov-excited-state-allowed and r.m.s.-radius-constraint regions do not overlap for a n^{20}C virtual energy larger than a keV (see [18]). Thus, while we cannot categorically rule out the existence of an Efimov state in ^{22}C, we can say that the ^{21}C system would need to be tuned very close to the unitary limit in order for an Efimov state to be present. Again, the results of [42] suggest that this is not the case, and so it appears highly doubtful that Efimov physics is realized in the ^{22}C nucleus. This is in accord with the conclusion of [43], where the three-body equations were solved for a variety of $2n$ halos assuming separable potentials for the nn and n–core interactions, and it was found that Borromean halo nuclei such as ^{22}C are less likely to provide realizations of the Efimov effect than the $2n$ halos where the corresponding $1n$ halo is also bound (e.g., ^{20}C).

5. Conclusion

Halo EFT is based on the premise that quantum systems which are loosely bound share universal features. This quantum universality has proven to be a very powerful way to correlate results in nuclear physics, atomic physics, and hadron physics [7,44]. In halo nuclei we have seen that there are universal formulae for, e.g., the $E1$ dissociation of an s-wave halo (eq. (2)) and the matter radius of an s-wave $2n$ halo. These encode correlations between experimental observables which occur purely because these are quantum bound states in which the particles spend most of their time outside the range of the interparticle potential. The resulting universal correlations should persist in $3n$ and $4n$ halos.

Of course, the applicability of a clustered description of these nuclei has long been recognized, and the degrees of freedom and general philosophy of EFT treatments of these reactions are the same as those in R-matrix and potential-model calculations. All such 'cluster models' use some data to fix parameters and then attempt to predict other observables. But the EFT's systematic expansion provides a quantitative estimate of the uncertainty at each order of approximation and a framework to improve accuracy.

As *ab-initio* calculations improve in power, accuracy, and scope one might question why any of these processes should not be computed directly. Part of the answer lies in the large separation of scales involved in such first-principles calculation: in the case of radiative proton capture on ^{7}Be the $E1$ integral must be carried out to 200 fm, and no *ab-initio* calculation should be used to describe physics on all scales from $\approx$1.5 fm to such a large distance. Indeed, much of any (low-energy) *ab-initio* reaction calculation amounts to an indirect treatment of the collective motion of clusters through and around

Coulomb and centrifugal barriers, and so Halo EFT can profitably be combined with *ab-initio* calculations. We are seeking to extend the LO calculations of captures in the $A = 8$ system to higher order, and we anticipate that additional information from *ab-initio* calculations will be needed if we want to continue to use the EFT to make predictions based largely on *ab-initio* input. Halo EFT has also been applied to ^{6}He [12,45] and this appears to be an excellent meeting ground for *ab-initio* calculations and Halo EFT – although in that case the formalism to make the connection remains to be worked out.

The combined insights gained from *ab-initio* calculations and Halo EFT will continue to illuminate the fascinating physics of the quantum few-body systems known as halo nuclei. In combination with data from existing and new facilities – particularly from facilities with unstable beams – this promises to significantly enhance our understanding of the interplay of nuclear dynamics and nuclear binding close to the drip line.

Acknowledgements

The author is grateful to the collaborators on the work reported in this paper, Hans-Werner Hammer, Bijaya Acharya, Xilin Zhang, Ken Nollett, and Chen Ji for enjoyable and productive collaborations, and to Chen and Ken in particular for useful comments on this manuscript. The author thanks the organizers of the International Symposium for their hospitality and for putting together a very interesting scientific programme. This work was supported by the US Department of Energy under Contract No. DE-FG02-93ER40756.

References

[1] D B Kaplan, M J Savage and M B Wise, *Phys. Lett. B* **424**, 390 (1998); *Nucl. Phys. B* **534**, 329 (1998)
[2] U van Kolck, *Nucl. Phys. A* **645**, 273 (1999)
[3] J Gegelia, *Phys. Lett. B* **429**, 227 (1998)
[4] M C Birse, J A McGovern and K G Richardson, *Phys. Lett. B* **464**, 169 (1999)
[5] S R Beane, P F Bedaque, W C Haxton, D R Phillips and M J Savage, From hadrons to nuclei: Crossing the border, in the Borris Ioffe Festschrift, *At the frontier of particle physics: Handbook of QCD* edited by M Shifman (World Scientific, Singapore, 2001), ISBN:981-02-4445-2
[6] P F Bedaque and U van Kolck, *Ann. Rev. Nucl. Part. Sci.* **52**, 339 (2002)
[7] H-W Hammer and L Platter, *Ann. Rev. Nucl. Part. Sci.* **60**, 207 (2010)
[8] C A Bertulani, H-W Hammer and U Van Kolck, *Nucl. Phys. A* **712**, 37 (2002)
P F Bedaque, H-W Hammer and U van Kolck, *Phys. Lett. B* **569**, 159 (2003)
[9] G Rupak and R Higa, *Phys. Rev. Lett* **106**, 222501 (2011)
L Fernando, R Higa and G Rupak, *Eur. Phys. J. A* **48**, 24 (2012)
[10] G Rupak, L Fernando and A Vaghani, *Phys. Rev. C* **86**, 044608 (2012)
[11] D L Canham and H Hammer, *Eur. Phys. J. A* **37**, 367 (2008); *Nucl. Phys. A* **836**, 275 (2010)
[12] J Rotureau and U van Kolck, *Few Body Syst.* **54**, 725 (2013)
[13] H-W Hammer and D R Phillips, *Nucl. Phys. A* **865**, 17 (2011)
[14] B Acharya and D R Phillips, *Nucl. Phys. A* **913**, 103 (2013)
[15] S Typel and G Baur, *Nucl. Phys. A* **759**, 247 (2005)
[16] X Zhang, K Nollett and D R Phillips, *Phys. Rev. C* **89**, 024613 (2014)

[17] K Tanaka *et al*, *Phys. Rev. Lett.* **104**, 062701 (2010)
[18] B Acharya, C Ji and D R Phillips, *Phys. Lett. B* **723**, 196 (2013)
[19] G Rupak, *Nucl. Phys. A* **678**, 405 (2000)
[20] C A Bertulani, arXiv:0908.4307 [nucl-th]
[21] T Nakamura *et al*, *Phys. Rev. Lett.* **83**, 1112 (1999)
[22] T Nakamura *et al*, *Nucl. Phys. A* **722**, 301 (2003)
[23] S Typel and G Baur, *Phys. Rev. C* **64**, 024601 (2001)
[24] D Bazin *et al*, *Phys. Rev. C* **57**, 2156 (1998)
[25] K M Nollett and R B Wiringa, *Phys. Rev. C* **83**, 041001 (2011)
[26] L Trache *et al*, *Phys. Rev. C* **67**, 062801(R) (2003)
[27] A D Gul'ko, S S Trostin and A Hudoklin, *Sov. J. Nucl. Phys.* **6**, 477 (1968)
[28] F C Barker, *Nucl. Phys. A* **588**, 693 (1995)
[29] J E Lynn, E T Jurney and S Raman, *Phys. Rev. C* **44**, 764 (1991)
[30] Y Nagai *et al*, *Phys. Rev. C* **71**, 055803 (2005)
[31] X Zhang, K M Nollett and D R Phillips, arXiv:1401.4482 [nucl-th]
[32] N Kobayashi *et al*, *Phys. Rev. C* **86**, 054604 (2012)
[33] M Langevin *et al*, *Phys. Lett. B* **150**, 71 (1985)
[34] P F Bedaque, H W Hammer and U van Kolck, *Phys. Rev. Lett.* **82**, 463 (1999)
[35] V Efimov, *Phys. Lett. B* **33**, 563
[35a] The binding energy of ^{22}C treated as a three-body system is equal to the two-neutron separation energy.
[36] S N Ershov, J S Vaagen and M V Zhukov, *Phys. Rev. C* **86**, 034331 (2012)
[37] M T Yamashita, L Tomio and T Frederico, *Nucl. Phys. A* **735**, 40 (2004)
[38] T Frederico, A Delfino, L Tomio and M T Yamashita, *Prog. Part. Nucl. Phys.* **67**, 939 (2012)
[39] M T Yamashita, R S M de Carvalho, T Frederico and L Tomio, *Phys. Lett. B* **697**, 90 (2011); Erratum, *ibid. B* **715**, 282 (2012)
[40] A Ozawa, O Bochkarev, L Chulkov, D Cortina, H Geissel, M Hellstrom, M Ivanov, R Janik *et al*, *Nucl. Phys. A* **691**, 599 (2001)
[41] D E Gonzales Trotter, F Salinas, Q Chen, A S Crowell, W Glockle, C R Howell, C D Roper, D Schmidt *et al*, *Phys. Rev. Lett.* **83**, 3788 (1999)
[42] S Mosby *et al*, *Nucl. Phys. A* **909**, 69 (2013)
[43] I Mazumdar, V Arora and V S Bhasin, *Phys. Rev. C* **61**, 051303 (2000)
[44] E Braaten and H-W Hammer, *Phys. Rep.* **428**, 259 (2006)
[45] C Ji, Ch Elster and D R Phillips, arXiv:1405.3294, submitted to *Phys. Rev. C*